Journal of Cerebral Blood Flow & Metabolism (2010) 30, 1188–1199

www.jcbfm.com

Increased plasma and tissue MMP levels are associated with BCSFB and BBB disruption evident on post-contrast FLAIR after experimental stroke

Ayush Batra[1,3,4,5], Lawrence L Latour[1,3], Christl A Ruetzler[2,3], John M Hallenbeck[2,3], Maria Spatz[3], Steven Warach[1,3] and Erica C Henning[1,3]

[1]*Stroke Diagnostics and Therapeutics Section, National Institute of Neurological Disorders and Stroke, National Institutes of Health, Bethesda, Maryland, USA;* [2]*Clinical Investigations Section, National Institute of Neurological Disorders and Stroke, National Institutes of Health, Bethesda, Maryland, USA;* [3]*Stroke Branch, National Institute of Neurological Disorders and Stroke, National Institutes of Health, Bethesda, Maryland, USA;* [4]*Howard Hughes Medical Institute—National Institutes of Health Research Scholars Program, Bethesda, Maryland, USA;* [5]*Cleveland Clinic Lerner College of Medicine, Case Western Reserve University, Cleveland, Ohio, USA*

In this study, we examined the relationship between tissue and blood levels of matrix metalloproteinase (MMP)-2 and MMP-9 through gelatin zymography at multiple time points after experimental stroke. We additionally investigated the association between these levels and the evidence of blood–cerebrospinal fluid (CSF) barrier (BCSFB) and blood–brain barrier (BBB) disruption on post-contrast fluid-attenuated inversion-recovery (FLAIR) imaging. Increased plasma MMP-9 was associated with BCSFB disruption at 1h post-reperfusion. Ventricular enhancement ipsilateral to the stroke was 500 ± 100%, significantly higher than sham, 24, and 48 h groups. Increased tissue MMP-2 and MMP-9 were associated with BBB disruption at 48 h post-reperfusion. Parenchymal enhancement was 60 ± 20% for a volume equivalent to 260 ± 80 mm³. Although the percent enhancement was comparable across groups, the volume of enhancing lesion was significantly higher at 48 h (260 ± 80 mm³, 100%) in comparison to 1 h (8 ± 3 mm³, 3%) and 24 h (51 mm³, 18%). These findings support the use of imaging markers of BCSFB and BBB status as indirect measures of MMP regulation in the blood and brain tissue. The methods presented herein should be useful in understanding the link between MMPs, barrier integrity, and subsequent hemorrhagic transformation.
Journal of Cerebral Blood Flow & Metabolism (2010) **30,** 1188–1199; doi:10.1038/jcbfm.2010.1; published online 3 March 2010

Keywords: blood–brain barrier; blood–CSF barrier; FLAIR; MMPs; MRI; stroke

Introduction

Matrix metalloproteinases (MMPs), members of the family of zinc-dependent endopeptidases, have a fundamental role in extracellular matrix physiology (Mun-Bryce and Rosenberg, 1998). MMPs are necessary for both extracellular matrix remodeling and the degradation of its protein components including collagen, laminin, and various proteoglycans (del Zoppo *et al*, 2007). Two specific MMPs, MMP-2 (gelatinase A) and MMP-9 (gelatinase B), have been the subject of extensive study in the stroke field given the ease with which they may be detected using zymography. There is growing evidence that both MMP-2 and MMP-9 are associated with blood–brain barrier (BBB) disruption and hemorrhagic transformation after ischemic injury (Heo *et al*, 1999; Montaner *et al*, 2001*b*; Rosenberg *et al*, 1996; Sumii and Lo, 2002). It has been suggested that MMP-2 is involved in early neuronal injury and delayed repair mechanisms, whereas MMP-9 is involved in increased vasogenic edema and subse-

Correspondence: Dr EC Henning, Section on Stroke Diagnostics and Therapeutics, Stroke Branch, National Institute of Neurological Disorders and Stroke, Building 10, Room B1D733, 10 Center Drive, MSC 1063, Bethesda, MD 20892, USA.
E-mail: henninge@ninds.nih.gov
Received 10 August 2009; revised 17 December 2009; accepted 28 December 2009; published online 3 March 2010

quent hemorrhage (Heo *et al*, 1999; Rosenberg *et al*, 1996). MMP-9 has also been associated with increased diffusion lesion volume and decreased neurologic outcome (Montaner *et al*, 2001*a*; Rosell *et al*, 2005).

Although this has generated widespread interest in the application of MMP inhibition for acute stroke therapy, our understanding of MMP regulation in the setting of acute ischemic insult and its impact on stroke progression remains limited. Studies using MMP-9 inhibition with synthetic inhibitors and tetracyclines have shown promise in their ability to reduce BBB disruption and final infarct volume if given in the acute phase (Murata *et al*, 2008; Nagel *et al*, 2008; Sood *et al*, 2008). However, long-term MMP inhibition leads to increased cortical damage, decreased neuroblast recruitment, and impaired recovery after ischemia (Lee *et al*, 2006; Sood *et al*, 2008; Zhao *et al*, 2006).

These seemingly contradictory findings stress the complex nature of MMPs and their multiphasic roles in stroke and brain injury (Rosell and Lo, 2008). Both the intravascular (blood) and extravascular (tissue) pools of MMPs have important implications to BBB disruption after ischemic stroke (Rosenberg, 2002). A limited number of experimental studies have aimed to understand the relationship between these two sources of MMPs (Heo *et al*, 1999; Nagel *et al*, 2008; Park *et al*, 2009). Heo *et al* (1999) reported increases in both tissue MMP-2 and MMP-9 within 2 h after stroke, but no such changes in plasma MMP-2 or MMP-9 (other than a transient increase in plasma MMP-9 at 2 h). In contrast, Nagel *et al* (2008) and Park *et al* (2009) reported parallel increases in both tissue and plasma MMP levels in the acute and subacute phases of stroke. At this time, the exact relationship between blood and tissue MMP levels and the mechanisms responsible for subsequent tissue injury remain ill defined. Since MMP blood biomarkers have the potential to serve as early prognostic indicators of stroke severity (i.e., infarct size, BBB disruption, risk of hemorrhage), this area warrants further investigation.

An imaging marker that may be used in conjunction with MMP biomarkers is HARM, or Hyperintense Acute reperfusion injuRy Marker (Latour *et al*, 2004). Enhancement visible on post-contrast fluid-attenuated inversion recovery (FLAIR) is thought to be indicative of blood–cerebrospinal fluid (CSF) barrier (BCSFB) and/or BBB disruption. This enhancement has been observed in CSF spaces such as the sulci and lateral ventricles, not the parenchyma (Henning *et al*, 2008*b*). Acute stroke, patients with the presence of HARM are at increased risk for hemorrhage and worse outcome, and HARM is more likely to be seen in patients treated with tissue plasminogen activator (tPA) (Warach and Latour, 2004). Given that FLAIR imaging is used routinely in stroke evaluation and has dramatically higher sensitivity for gadolinium enhancement versus standard T_1 imaging (Mamourian *et al*, 2000), the comparison of pre-contrast and post-contrast FLAIR should provide a reliable and relatively noninvasive method for determining BCSFB-BBB status.

In this study, we had two major aims. First, we wanted to examine the relationship between blood plasma and brain tissue levels of MMP-2 and MMP-9 at various time points after transient middle cerebral artery occlusion (MCAO). Second, we were interested in determining the associations (if any) between these MMP levels and the extent of BCSFB and BBB disruption observed on post-contrast FLAIR. This project is unique in associating the time course of MMP expression present within the blood and tissue with clinically used imaging protocols during the acute and subacute time window after ischemic stroke. We hypothesize that elevated levels of MMPs in the blood/tissue are associated with barrier disruption evident on post-contrast FLAIR. These methods should be useful in understanding the link between MMPs and vascular integrity, and may be extended to monitor efficacy of therapeutic intervention such as MMP inhibition.

Materials and methods

Animals

This study was approved by the Institutional Animal Care and Use Committee of the National Institute of Neurological Disorders and Stroke, National Institutes of Health (IACUC protocol No. 1225-08). Thirty-four male spontaneously hypertensive (SHR) rats (SHR/NCrl, 3 to 4 months old, 335 to 375 g, systolic blood pressure 165 to 185 mm Hg; Charles River Laboratories, White Plains, NY, USA) were anesthetized with 2.5% isoflurane delivered in a mixture of nitrogen, medical-quality air, and oxygen (2:2:1 ratio). Animals were divided into five experimental groups: naive, sham, 1, 24, and 48 h. Animals within the naive group did not undergo surgery or imaging and were strictly used as tissue and plasma sample controls. Sham-operated animals underwent right femoral vein and artery catheterization along with the full imaging protocol described below. All animals within the 1, 24, and 48 h groups underwent femoral vein and artery catheterization followed by 45 mins of transient right MCAO via the intraluminal suture model.

Middle Cerebral Artery Occlusion

Middle cerebral artery occlusion was performed using the methods first described by Koizumi *et al* (1986) and later modified by Longa *et al* (1989). The right common carotid artery, internal carotid artery, and external carotid artery (ECA) were exposed through a midline incision of the neck. The superior thyroid artery and occipital artery were double ligated (5-0 braided silk suture; Roboz Surgical Instruments, Gaithersburg, MD, USA) and cut to isolate the ECA. The ECA was double ligated (4-0 braided silk suture; Roboz) ~1 cm distal to the bifurcation. The ECA was flipped parallel to the internal carotid artery after dissec-

tion, and the common carotid artery was clamped for preparation of suture insertion. A 3-0 nylon suture (#663H, Ethilon FS-1, Henry Schein, Melville, NY, USA) with a heat-rounded, silicone-coated tip (Provil Novo Light; Heraeus-Kulzer Inc., South Bend, IN, USA) was inserted and advanced via the ECA into the internal carotid artery. Mild resistance was felt at a distance of ~19 mm from the MCA-ACA bifurcation, indicating successful occlusion of the MCA. After 45 mins, the suture was removed and the ECA was permanently ligated (4-0 braided silk suture, Roboz). Blood flow was then reestablished via the common carotid artery by removing the clamp.

Magnetic Resonance Imaging

Magnetic resonance imaging (MRI) was performed with a 7.0-T/30-cm imaging spectrometer (Bruker Biospin, Billerica, MA, USA) immediately after sham or MCAO surgery. Animals in the sham, 1, 24, and 48 h groups were imaged with gradient-echo imaging (GRE) and diffusion-weighted, echo-planar imaging (DW-EPI) to evaluate the presence/absence of hemorrhage and the presence of stroke at baseline (30 mins after occlusion). Final imaging was performed immediately after reperfusion for the 1h group, 24 h post-reperfusion for the 24 h group, and 48 h post-reperfusion for the 48 h group. Animals were imaged with two GREs (one low resolution, one high resolution), DW-EPI, FLAIR, and T2. Animals were given a 0.2-mL intravenous bolus of Gd-DTPA (Magnevist, Berlex Laboratories, Wayne, NJ, USA) and imaged post-contrast with an additional DW-EPI, FLAIR, and T2. Post-contrast FLAIR scans were standardized to be exactly 10 mins after bolus injection. Figure 1 details the imaging design, along with the blood/tissue collection and neurologic scoring.

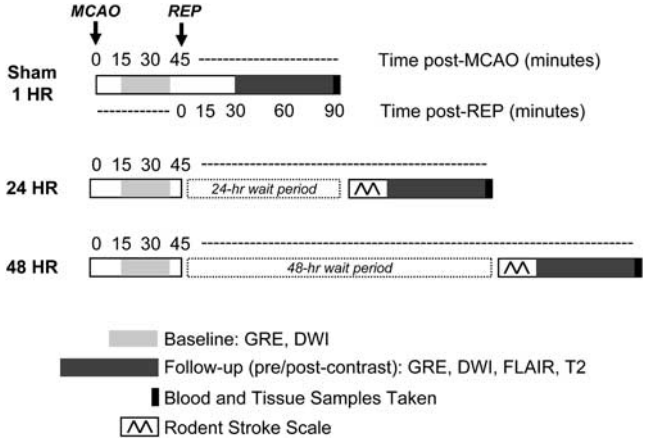

Figure 1 Experimental design. Imaging experiments were performed according to the above timeline. Animals were separated into five groups (naive, sham, 1, 24, 48 h groups). Naive animals received no imaging and were strictly used as blood and brain tissue controls. All remaining animals received a baseline scan 30 mins after sham surgery or MCAO. Follow-up imaging was performed immediately after reperfusion (REP) for sham and 1 h groups, at 24 h for the 24 h group, and at 48 h for the 48 h group. Blood and brain tissue samples were taken immediately after final imaging.

For all imaging, a localizer tripilot was acquired and the front edge of the slice package was placed at the level of the olfactory bulb. Twelve 1.5 mm-thick slices were acquired with a field of view of $2.56 \times 2.56\,cm^2$. DW-EPI was performed using TR/TE = 6200/46 ms, 6 b values (250 → 1500 s/mm^2), and 8 averages. FLAIR was performed using TR/TE/TI = 10000/48/1600 ms, rare factor = 8, and 2 averages. T2 was performed using TR = 2000 ms, 8 echo times (15 → 120 ms), and 1 average. The GRE (low resolution) was performed using 12, 1.5 mm-thick slices, TR/TE = 300/12 ms and 2 averages. The GRE (high resolution) was performed using 18, 1.0 mm-thick slices, TR/TE = 360/12 ms, and 4 averages. In-plane resolutions were 267 μm for DW-EPI, 200 μm for FLAIR and T2, and 100 μm for GRE.

Inclusion/Exclusion Criteria

Animals were excluded from the study if the GRE showed the presence of subarachnoid hemorrhage or the diffusion lesion volume was $< 50\,mm^3$, suggesting surgical error due to improper suture placement at time of MCAO.

Neurologic Scoring

Animals were monitored daily for activity, appearance, gait, appetite, hydration, and weight after MCAO. The 'Rodent Stroke Scale,' a modification of the method developed originally by Garcia *et al* (1995), was performed once before final imaging for animals within the 24 and 48 h groups. Animals were scaled for spontaneous activity (0 to 3), symmetry of movements (0 to 3), forepaw outstretching (0 to 3), climbing (1 to 3), body proprioception (1 to 3), and response to touch (1 to 3) with 18 representing a perfect neuroscore assessment.

Blood and Tissue Collection

Blood and tissue samples were collected within 15 mins after the final imaging sequence while the animals were under 3% to 4% isoflurane anesthesia. A total of 6 mL of blood was collected via transcardial puncture in three 2-mL Vacutainer sodium-citrate tubes (Becton Dickinson, Franklin Lakes, NJ, USA) and immediately placed on ice. Samples were centrifuged for 30 mins at 2,000 g within 1 h of blood collection. Plasma samples were collected, aliquoted, and stored at −80°C. After blood collection, animals underwent transcardial perfusion with 100 mL ice-cold phosphate-buffered saline. Animals were decapitated and brain tissue was dissected on ice. Brains were hemisectioned into ischemic and nonischemic sides, flash frozen in 2-methylbutane, and stored at −80°C. Cerebellum samples were discarded before sample freezing.

Image Analysis

User-defined routines written in IDL software (Version 7.0, Research Systems Inc, Boulder CO, USA) were used to perform all MRI analysis and produce all parameter maps (apparent diffusion coefficient (ADC), T2). Volumes of

interest (VOIs) were drawn using MIPAV software (Biomedical Imaging Research Services Section, National Institutes of Health, Bethesda, MD, USA). Lesion severity was quantified based on ADC hypointensity and T2 hyperintensity. Individual VOIs were drawn for ischemic lesion and contralateral healthy tissue on ADC and T2 maps. Lesion volume, average ADC, average T2, and gross edema (right versus left hemisphere) were calculated. Barrier disruption (BCSFB, BBB) was quantified based on a change in signal intensity from pre-contrast FLAIR to post-contrast FLAIR, with normalization by pre-contrast values. The presence of HARM, or gadolinium enhancement of the CSF spaces, was assessed by monitoring the signal of the ipsilateral (right) and contralateral (left) ventricles. Individual VOIs were drawn for the lateral ventricles on pre-contrast FLAIR, with projection to post-contrast time points. The presence of BBB disruption, or gadolinium enhancement of the parenchyma, was assessed by identifying parenchymal enhancement on post-contrast FLAIR. Individual VOIs were drawn for positive, enhancing regions. VOIs for nonenhancing regions were calculated by subtracting enhancing regions from lesion VOIs. Volume and percent enhancement were calculated.

Gelatin Zymography

Gelatin zymography was performed to determine the relative levels and activity of MMP-2 and MMP-9 in plasma samples and hemispheric brain tissue. On study initiation, we used purified mouse recombinant MMP-2 and MMP-9 (gift from Christina Stuelten, PhD, National Cancer Institute, National Institutes of Health) to verify individual MMP band locations in comparison to a standard protein ladder (SeeBlue Pre-Stained Standard, Invitrogen, Carlsbad, CA, USA). Subsequent experiments included running the standard protein ladder and a bacterial collagenase control (2 ng) adjacent to plasma and tissue samples. These allowed for determination of band locations and molecular weights, as well as standardization of gelatin activity.

For plasma samples, total protein concentrations were determined through the BCA protein assay and samples were diluted to concentrations of 10 μg/μL in CHAPs lysis buffer (50 mmol/L Tris-HCL (pH 7.6), 150 mmol/L NaCl, 5 mmol/L $CaCl_2$, and 0.05% BRIJ-35). Each lane was loaded with 50 μg total plasma protein in a 1:1 ratio with loading buffer (90 mmol/L Tris-HCL (pH 6.8), 4% SDS, 10% glycerol, and 0.01% bromophenol blue) and samples were separated through electrophoresis on 10% polyacrylamide gels containing 0.1% gelatin (Invitrogen). Gels were incubated in renaturing buffer (Invitrogen) for 30 mins, and then treated in developing buffer (Invitrogen) for 30 mins. Gels were incubated for 48 h at 37°C in fresh developing buffer with gentle agitation. Gels were stained with 0.5% Coomassie Blue R-250 (Invitrogen), destained, and imaged using Fluor Chem (Alpha Innotech, San Leandro, CA, USA).

For hemispheric brain tissue, samples were homogenized in lysis buffer and centrifuged at 4°C for 15 mins at 6,000 *g*. Supernatants were collected and total protein concentrations were determined through the BCA protein assay. Samples were diluted to concentrations of 10 μg/μL in lysis buffer. Tissue gelatinase levels were assessed using gelatin sepharose purification (Zhang and Gottschall, 1997). A total of 50 μL of prewashed gelatin Sepharose 4B (GE Healthcare Bio-Sciences Corp, Pittsburgh, PA, USA) diluted 1:1 in sample with lysis buffer was incubated for 60 mins with constant agitation. Samples were centrifuged for 5 mins at 5,000 *g*. The pellet was resuspended in 500 μL of lysis buffer and centrifuged for a second time at 5,000 *g* for 5 mins. The pellet was isolated, resuspended in lysis buffer containing 10% DMSO, and incubated for 30 mins. Samples were centrifuged for 5 mins at 5,000 *g*. The supernatant was collected, 10 μL of which was mixed with 10 μL of loading buffer. Each lane was loaded with 20 μL of sample/loading buffer, and the samples were separated through electrophoresis on 10% polyacrylamide gels containing 0.1% gelatin (Invitrogen). Gels were processed in the same manner as described earlier.

Band intensities of total MMP-9 and total MMP-2 (pro and active forms) were quantitatively determined by the Spot-denso-program with Alpha Ease software (Alpha Innotech). Separate measurements, when possible, were made for pro and active forms in order for comparison with total MMP levels. Results were reported as the average integrated density value (IDV) ratios obtained by standardizing each band to the intensity of the collagenase control.

Enzyme Immunohistochemistry

Enzyme immunohistochemistry was performed with one brain tissue sample from each experimental group (naive, sham, 1, 24, 48 h). Rat IgG staining was performed to assess BBB disruption in comparison to post-contrast FLAIR findings. MMP staining was performed to localize potential sources of MMP-2 and MMP-9 increase. Additional cresyl violet staining was performed to differentiate infarct from healthy tissue and morphological changes in the choroid plexus.

For MMP-2 and rat IgG, 16 μm sections of fresh frozen rat brains were post-fixed in 4% paraformaldehyde for 10 mins. For MMP-9, sections were post-fixed in acetone for 5 mins. Permeabilization was performed with 0.3% TWEEN/phosphate-buffered saline for 1 h. Endogenous peroxide was blocked with 0.3% hydrogen peroxide in methanol for 20 mins. Sections were incubated in 5% NDS for 1 h, followed by overnight incubation with primary polyclonal antibodies against rat MMP-2 (1:100; Millipore, Billerica, MA, USA), rat MMP-9 (1:100, Millipore), or rat IgG (1:2000; Jackson Labs, West Grove, PA, USA). Negative control sections were prepared with rabbit IgG (1:2000, Jackson Labs) for MMP-2 and MMP-9. Sections were incubated for 1 h with secondary antibody (donkey anti-rabbit or anti-rat, 1:2000; Jackson Labs). Sections were developed using VECTASTAIN ABC Kit (Vector Labs, Burlingame, CA, USA) and antibody-binding sites were visualized with diaminobenzidine (DAB Kit, Sigma, St Louis, MO, USA).

Statistical Analysis

All statistical analyses were performed using SPSS. Data are presented as mean ± s.d. Graphs are presented using mean ± standard error of the mean (s.e.m.). Data was tested

for normality using a Shapiro-Wilk test. For lesion and MMP analyses, normally distributed data sets were compared using one-way between-groups ANOVA with *post hoc* comparisons using Tukey. Nonnormal data sets were compared using Kruskal–Wallis with *post hoc* comparisons using Mann–Whitney. For FLAIR signal analyses, data sets were compared using independent samples *t*-tests or Wilcoxon-signed Rank, depending on normality conditions. For all analyses, $P<0.05$ was considered to be significant.

Results

Group Characteristics

GRE images were used to exclude three animals (two within the 24 h group and one within the 48 h group) based on the presence of subarachnoid hemorrhage after MCAO, most likely due to surgical error. One additional animal was excluded from the 48 h group due to premature death, attributed to an exceptionally large infarct (volume $>300\,mm^3$) and brain herniation. This resulted in a final $N=6$ per group.

There were no significant differences across groups (naive, sham, 1, 24, 48 h) for average weight, MCAO time, and surgical vitals. Average MCAO time between the 1, 24, and 48 h groups was 49 ± 3 mins. There was a significant difference in anesthesia time for sham versus 1, 24, and 48 h groups ($P<0.05$). A detailed description of all physiological parameters in addition to tissue collection times is shown in Table 1.

The 24 h group had a mean neurologic score of 14 ± 1, whereas the 48 h group had a mean neurologic score of 13 ± 1. This difference was not statistically significant ($P=0.22$).

Magnetic Resonance Imaging Lesion Evolution

Baseline ADC lesion volumes showed no significant differences among groups after MCAO ($P=0.11$). Average lesion volumes were $270\pm30\,mm^3$. Follow-up ADC lesion volume for the 1 h group was $30\pm40\,mm^3$, significantly smaller than baseline ($P<0.05$). Follow-up T2 lesion volumes were comparable for 24 and 48 h groups ($240\pm50\,mm^3$ and $260\pm50\,mm^3$, $P=0.38$). Lesion T2 values were significantly higher within the 48 h group compared with the 24 h group (88 ± 6 ms versus 80 ± 3 ms, $P<0.05$). Similarly, gross edema and midline shift seemed to be higher within the 48 h group compared with the 24 h group ($17\pm5\%$ versus $12\pm3\%$, $P<0.06$).

Magnetic Resonance Imaging of Blood–Cerebrospinal Fluid and Blood–Brain Barrier Disruption

Barrier status (BCSFB, BBB) was assessed through FLAIR imaging with and without gadolinium contrast (Figure 2). For the sham group, post-contrast FLAIR images were considered negative. For the 1 h group, all animals (6 of 6) showed evidence of CSF enhancement. Ventricular enhancement ipsilateral to the stroke was $500\pm100\%$, significantly higher than sham, 24, and 48 h groups ($P<0.01$). Ventricular enhancement contralateral to the stroke was $30\pm10\%$, significantly higher than sham ($P<0.05$), but comparable to 24 and 48 h groups ($P\geq0.19$). For the 48 h group, all animals (6 of 6) showed dramatic parenchymal enhancement encompassing the entire infarct region. Parenchymal enhancement was $60\pm20\%$ for a volume equivalent to $260\pm80\,mm^3$ ($100\pm20\%$ of T2 lesion volume). Although the percent enhancement was comparable across groups ($P\geq0.37$), the volume of enhancing lesion was significantly higher for the 48 h group ($260\pm80\,mm^3$, 100%, $n=6$) in comparison to the 1 h ($8\pm3\,mm^3$, 3%, $n=3$) and 24 h (51 mm^3, 18%, $n=2$) groups ($P<0.01$). A detailed description of FLAIR signal changes for CSF spaces and parenchyma is provided in Table 2.

Table 1 Physiological parameters for experimental groups (sham, 1, 24, 48 h)

	Sham	*1 h*	*24 h*	*48 h*	P *value*
Group demographics					
Animal weight (g)	363 (9)	350 (10)	350 (10)	348 (6)	0.09
Total anesthesia time (h to mins)	2 h20 m (10 m)#	3 h50 m (20 m)	3 h40 m (30 m)	3 h30 m (20 m)	#<0.05
MCA occlusion time (mins)	n/a	50 (4)	48 (3)	48 (2)	0.42
Tissue collection time (time post-reperfusion)	n/a	1 h38 m (8 m)#	25 h (1 h)#	47 h (2 h)#	#<0.01
Surgical vitals					
Heart rate (beats/min)	300 (10)	310 (10)	300 (10)	310 (10)	0.22
Temperature (°C)	37.1 (0.4)	37.3 (0.2)	36.9 (0.3)	37.1 (0.4)	0.48
Oxygen saturation (spO_2)	87 (3)	90 (2)	90 (1)	91 (4)	0.07
Vaporizer level (% isoflurane)	2.7 (0.1)	2.6 (0.1)	2.6 (0.1)	2.6 (0.1)	0.29

Values are expressed as mean (s.d.). Naive animals received no surgery or imaging and served as a control group. Naive animals had a weight of 350 g (10), which was not significantly different than other groups.
#Significance versus all other groups.

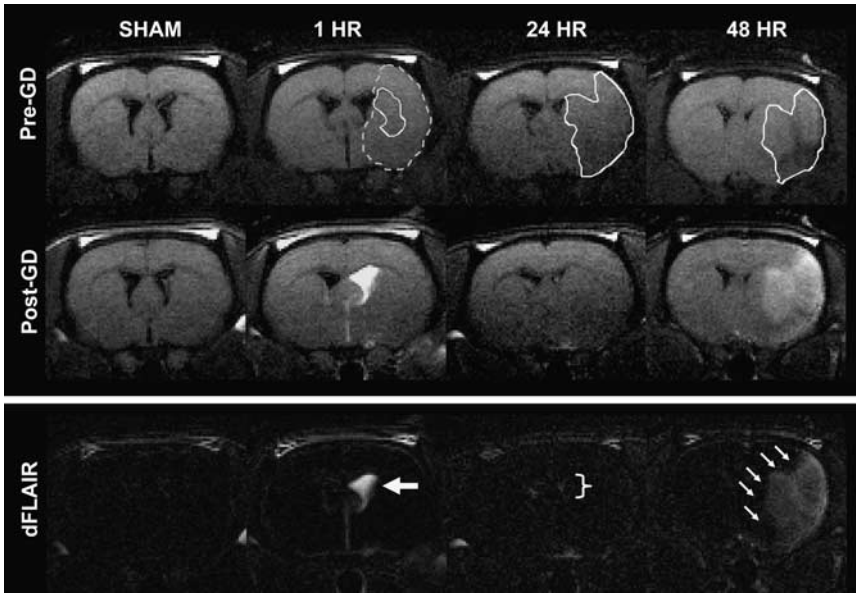

Figure 2 FLAIR imaging of barrier disruption. Blood–CSF barrier (BCSFB) and blood–brain barrier (BBB) disruption were quantified through FLAIR MRI with and without Gd-DTPA. The outlined region (dotted line) for the 1 h group represents the ADC lesion at baseline before reperfusion. The outlined regions (solid lines) represent the ADC lesion for the 1 h group and T2 lesion for the 24 and 48 h groups post-reperfusion. Post-Gd FLAIR scans were standardized to be exactly 10 mins after Gd-DTPA administration. The 1 h group showed evidence of BCSFB disruption (large arrows) on post-Gd FLAIR and dFLAIR (difference map, pre-Gd versus post-Gd). Ventricular enhancement ipsilateral to the stroke was 500 ± 100%, significantly higher than sham, 24 (bracket), and 48 h groups ($P < 0.01$). The 48 h group showed evidence of BBB disruption (small arrows) on post-Gd FLAIR and dFLAIR (difference map, pre-Gd versus post-Gd). Parenchymal enhancement present throughout the infarct was 60 ± 20% for a volume equivalent to 260 ± 80 mm^3 (100 ± 20% of T2 lesion volume). This was significantly higher than both 1 and 24 h groups ($P < 0.01$).

Table 2 FLAIR signal evolution for experimental groups (sham, 1, 24, 48 h)

	Sham	*1 h*	*24 h*	*48 h*	P *value*
Ventricles					
Ipsilateral (right) (% relative to pre-contrast)	10 (10)	500 (100)#*	60 (20)*	40 (10)*	#<0.01 *<0.05
Contralateral (left) (% relative to pre-contrast)	10 (10)	30 (10)*	33 (10)*	25 (6)*	*<0.05
Parenchyma					
Nonenhancing lesion (% relative to pre-contrast)	1 (4)	10 (4)*	14 (4)*	13 (3)*	*<0.05
Enhancing lesion (% relative to pre-contrast)	n/a	60 (30)	38	60 (20)	≥0.37
Size of enhancing lesion (mm^3)	n/a	8 (6)	51	260 (80)#	#<0.01
Size of enhancing lesion (%)	n/a	3 (2)	18	100 (20)#	#<0.01

Values are expressed as mean (s.d.).
*Significance versus sham, #Significance versus all other groups.

Gelatin Zymography

Plasma zymography showed a consistent presence of three distinct MMP bands—pro-MMP-9 (92 kDa), pro-MMP-2 (72 kDa), and active-MMP-2 (64 kDa) (Figure 3). Active MMP-9 (82 kDa) was observed in 50% (3 of 6) of the plasma samples. Plasma levels of total MMP-9 were significantly increased within the 1 h group in comparison to naive ($P < 0.01$). This was comparable to the increase in pro-MMP-9 within the 1 h group in comparison to naive ($P < 0.01$), 24 h ($P < 0.05$), and 48 h ($P < 0.01$) groups. There appeared to be no change in active MMP-9. Plasma levels of total MMP-2 showed a decreasing trend from the naive group to the 48 h group, but the differences were not significant ($P = 0.09$). Similarly, there were no changes in plasma levels of pro-MMP-2 ($P = 0.08$) or active-MMP-2 ($P = 0.18$).

Brain tissue zymography showed a consistent presence of two distinct MMP bands—pro-MMP-9 (92 kDa) and active-MMP-2 (64 kDa) (Figure 4). Active-MMP-9 (82 kDa) was observed in 80% (4 of 5) of brain tissue samples. Discrete bands for pro-MMP-2 (72 kDa) were weak and difficult to discern from strong active-MMP-2 bands. Brain tissue levels of total MMP-9 were significantly increased within

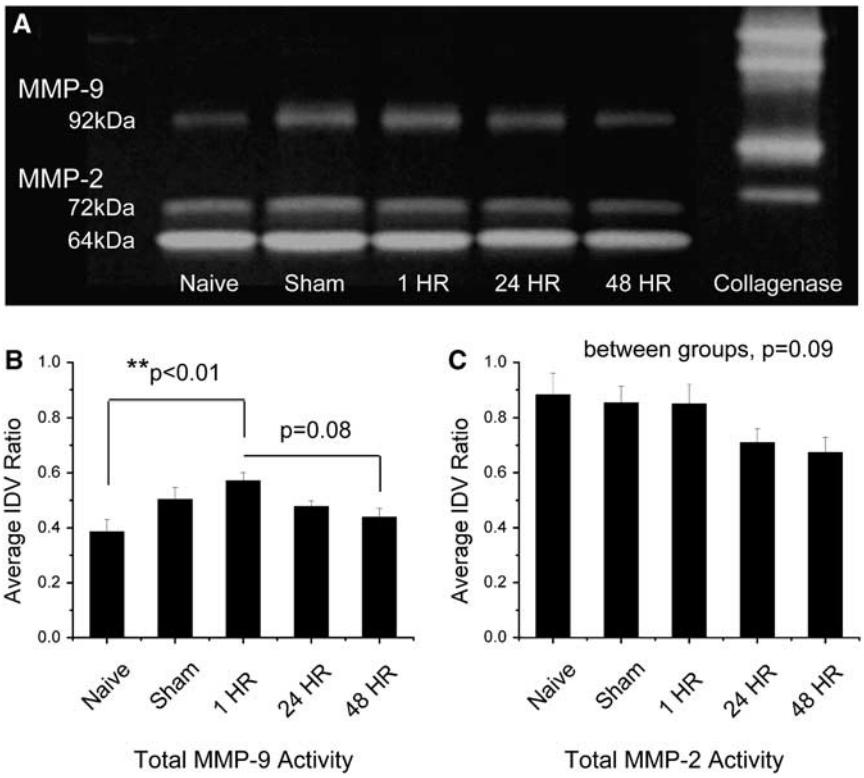

Figure 3 Plasma zymography. (**A**) Representative zymogram comparing plasma MMP-2 and MMP-9 levels across naive, sham, 1, 24, and 48 h groups. A bacterial collagenase control was used to standardize band intensities across gels. (**B**) Quantified densitometry of total MMP-9 (pro + active). MMP-9 levels were increased within the 1 h group in comparison to the naive group. (**C**) Quantified densitometry of total MMP-2 (pro + active). There were no changes in MMP-2 levels. Values are presented as mean ± standard error of the mean (s.e.m.). $N = 6$ for individual groups. $^{**}P < 0.01$.

the 48 h group in comparison to naive, sham, and acute groups ($P < 0.01$). This increase was comparable between the 24 and 48 h groups ($P = 0.38$). These findings were consistent with the increase in pro-MMP-9 within the 48 h group in comparison to naive, sham, and acute groups ($P < 0.05$). Pro-MMP-9 levels were similar between the 24 and 48 h groups ($P = 0.32$). There appeared to be an increasing trend in active MMP-9 from the naive group through the 48 h group, but differences were not significant ($P = 0.13$). Brain tissue levels of total MMP-2 were significantly increased within the 48 h group in comparison to all others ($P < 0.05$). The majority of this change may be attributed to the active rather than pro form of MMP-2.

Enzyme Immunohistochemistry

For the 1 h group (Figure 5, black asterisks), the ipsilateral ventricle and choroid plexus showed intense cytoplasmic vacuolization (swelling), indistinct epithelial membranes, and varying degrees of pyknosis. MMP-2 staining was almost nonexistent, whereas MMP-9 staining was increased in comparison to sham. The morphological changes observed at 1 h were less obvious for the 24 and 48 h groups, suggesting partial recovery. Observed staining for MMPs seemed to be localized to the choroid epithelia (MMP-2/9), the stroma (MMP-2), and infiltrating macrophages (MMP-9).

For the 48 h group (Figure 5, yellow asterisks), the lesion core showed frank necrosis, intense IgG staining with perivascular extension into the parenchyma, and MMP-2 and MMP-9 staining of vessels, microglia, and macrophages. Further positive staining included a limited number of neurons. Similar observations were made along the lesion periphery. The changes observed at 48 h group were more severe than both the 1 and 24 h groups. IgG extravasation and MMP-9 staining were not evident in the naive or sham groups. A base level of MMP-2 staining was present in naive and sham groups, and included vessels, astrocytes, and a limited number of neurons.

Discussion

Although in animal studies we are able to measure MMP levels in the blood and brain tissue, clinical studies rely heavily on blood levels as surrogate markers for MMP activity in the brain. To clinically utilize MMP blood biomarkers to track stroke progression and outcome, a link between MMPs in the blood and brain, as well as subsequent tissue

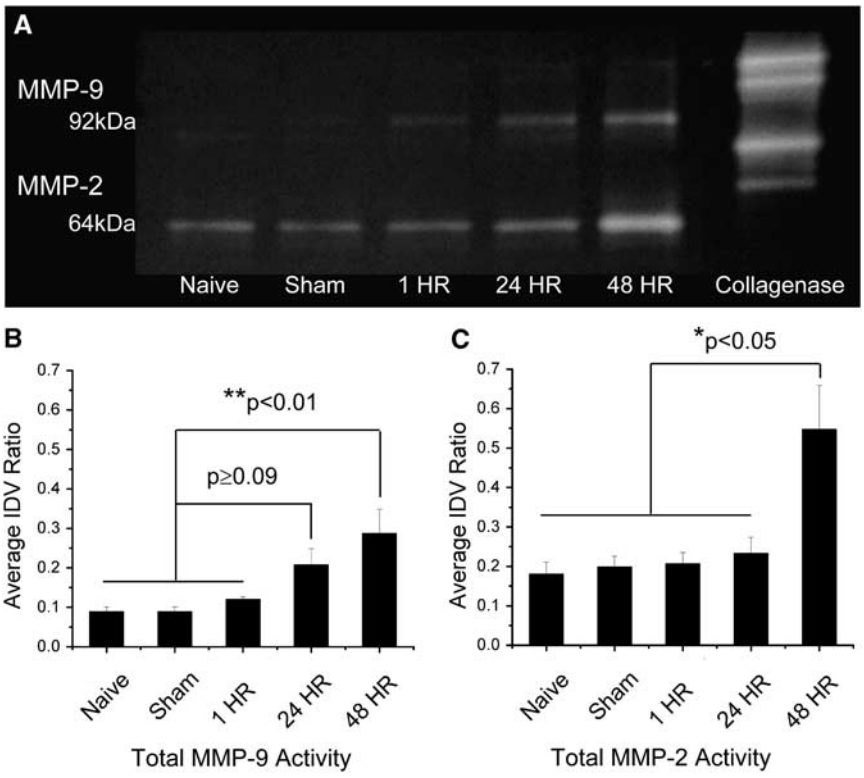

Figure 4 Brain tissue zymography. (**A**) Representative zymogram comparing brain tissue MMP-2 and MMP-9 levels across naive, sham, 1, 24, and 48 h groups. A bacterial collagenase control was used to standardize band intensities across gels. (**B**) Quantified densitometry of total MMP-9 (pro + active). MMP-9 levels were increased for the 48 h group in comparison to naive, sham, and 1 h groups. (**C**) Quantified densitometry of total MMP-2 (pro + active). MMP-2 levels were increased for the 48 h group in comparison to all others. Values are presented as mean ± standard error of the mean (s.e.m.). $N = 5$ for individual groups. $*P < 0.05$, $**P < 0.01$.

injury, must be provided. In this study, we were able to show that the pattern of release of MMPs in the blood differs significantly from that in brain tissue. In addition, we identified two distinct patterns of barrier disruption using post-contrast FLAIR imaging—BCSFB and BBB disruption. We found (1) an association between increased plasma MMP-9 and BCSFB disruption (HARM) at 1 h post-reperfusion and (2) an association between increased tissue MMP-2 and MMP-9 and BBB disruption at 48 h post-reperfusion.

Post-contrast FLAIR imaging of animals within the 1 h group revealed an interesting pattern of barrier disruption. Ventricular enhancement ipsilateral to the stroke within 1 h post-reperfusion suggests that the BCSFB may be disrupted immediately after ischemic insult. This pattern of enhancement has been described previously using post-contrast T1-weighted imaging in both permanent MCAO models and delayed reperfusion models (Kastrup *et al*, 1999; Nagahiro *et al*, 1994), but never so early after ischemic injury. Visualizing this pattern of disruption with post-contrast FLAIR imaging is a novel finding of our study. By 24 h, this enhancement was significantly diminished, suggesting partial but incomplete recovery of the choroid plexus after ischemia-reperfusion injury (Ennis and Keep, 2006; Johanson *et al*, 2000). Although not as readily investigated in stroke, the choroid plexus is directly involved in communication between the brain, vasculature, and CNS. The choroid responds immediately to peripheral inflammatory signals within the blood through chemokine signaling, expression of pro-inflammatory cytokines, and alterations in tight junction proteins (Mitchell *et al*, 2009). With time, the choroid plexus is able to regulate and maintain BCSFB integrity through correction of fluid-electrolyte imbalances (Palm *et al*, 1995). The choroid is also able to promote tissue repair through expression of a variety of growth factors in response to autocrine and paracrine signaling mechanisms (Johanson *et al*, 2000).

Post-contrast FLAIR imaging of animals within the 48 h group, but not the 1 or 24 h group, showed parenchymal enhancement encompassing the entire infarct region. These observations indicate widespread BBB disruption at 48 h, consistent with Gd-DTPA extravasation and shortening of local tissue T1 observable based on inversion-recovery preparation within the FLAIR sequence. Animals in the 48 h group had significant vasogenic edema and elevated lesion T2 values. We observed similar increases in lesion T2 values in the 24 h group; however, this group did not have significant parenchymal en-

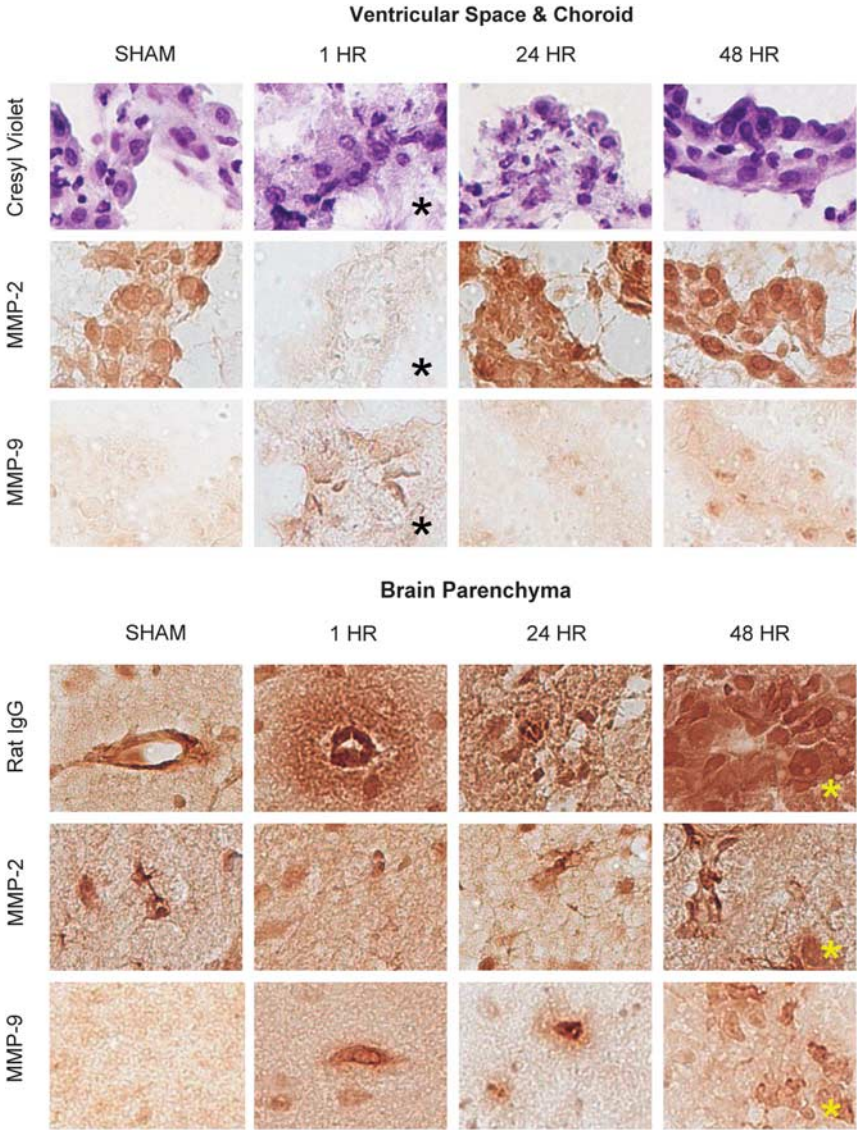

Figure 5 Enzyme immunohistochemistry. Images (40 ×) of representative brain tissue from sham, 1, 24, and 48 h groups. Top: ventricles and choroid plexus. For the 1 h group (black asterisks), cresyl violet staining showed intense cytoplasmic vacuolization (swelling), indistinct epithelial membranes, and varying degrees of pyknosis. MMP-2 staining was almost nonexistent, whereas MMP-9 staining was increased in comparison to sham. The morphological changes observed at 1 h were less obvious for the 24 and 48 h groups, suggesting partial recovery. Bottom: brain parenchyma. For the 48 h group (yellow asterisks), the lesion core showed frank necrosis, intense IgG staining with perivascular extension into the parenchyma, and MMP-2 and MMP-9 staining of vessels, microglia, and macrophages. Further positive staining included a limited number of neurons. Similar observations were made along the lesion periphery. The changes observed at 48 h were more severe than both the 1 and 24 h groups.

hancement. It is entirely possible that for the 24 h group, the barrier is relatively intact, but the ability of the endothelial cells to maintain normal ionic gradients is compromised (Simard *et al*, 2007). Following the failure of ionic homeostasis, widespread vasogenic edema occurs with compromised BBB integrity and Gd-DTPA extravasation. The GRE images revealed hemorrhagic transformation along the infarct periphery in one animal (16.7%) at 24 h and two animals (33.3%) at 48 h. Recent work in SHR, having comparable infarct volumes and T2 values to this study, showed that 84.6% of animals hemorrhage by day 3, with a 100% incidence by day 7 (Henning *et al*, 2008*a*). These findings support previously reported associations between BBB disruption and hemorrhage post-stroke (Hamann *et al*, 1996; Heo *et al*, 1999; Sumii and Lo, 2002). It is likely that changes in microvascular integrity begin at the interface between astrocytes, the extracellular matrix, and the basal lamina (Hamann *et al*, 1996; Milner *et al*, 2008). Degradation of components of the basal lamina, such as laminin and collagen type IV, have been linked to diapedesis of blood and the formation of petechial hemorrhage (Hamann *et al*,

1995, 1996). Further study is warranted to investigate the mechanisms involved in vascular compromise and the threshold of microvascular damage required for hemorrhagic transformation.

It is important to point out that lesions were not visualized on pre-contrast FLAIR images within the 24 and 48 h groups due to the T1-weighted nature of the FLAIR sequence. Instead, lesions were identified on standard T2. At high field (7 T), to obtain appropriate CSF signal suppression without sacrificing brain tissue signal-to-noise, a T1-weighted FLAIR sequence with an intermediate TE (48 ms) was used. This does not allow for lesion identification at high field (7 T), in contrast to lower field strengths (1.5 T or 3 T), which are able to use T2-weighted FLAIR sequences at long TEs (120 ms). Regardless of the exact weighting of the FLAIR sequence, suppression of the CSF signal permits accurate and reliable delineation between CSF and parenchyma, and greater sensitivity to any enhancement that is observed post-contrast (Mamourian *et al*, 2000).

The noted IgG extravasation supports the pattern of BBB disruption observed on post-contrast FLAIR imaging at 24 and 48 h, but not at 1 h. IgG extravasation in the 1h group was contradictory to the relative absence of parenchymal enhancement at that time point. This is consistent with prior work by Lo *et al* (1994). This discrepancy may be due to multiple factors. First, depending on the status of the BBB, endogenous IgG may extravasate during the entire occlusion period and through 1 h post-reperfusion. Gd-DTPA, however, is given only at 1h post-reperfusion, with BBB assessment 10 mins after administration of contrast. The timing of these two methods does not match, so it is not surprising that we observed differences in technique sensitivity. Second, the mechanisms of IgG extravasation and Gd-DTPA extravasation remain poorly understood. If they occur via different mechanisms, such as receptor-mediated endocytosis versus passage through nonfunctional tight junctions, the patterns of enhancement observed would not match. Third, immunohistochemistry is inherently more sensitive than MRI based on a 10 to 100-fold difference in spatial resolution. Although a post-contrast FLAIR image may be read as 'negative,' it is likely that there are vascular changes occurring not observable by MRI. To overcome some of these issues, an intravenous injection of Gd-DTPA mixed with fluorescently tagged IgG may serve as a better correlate between imaging findings and tissue immunohistochemistry.

Early increases in plasma MMP-9 were present within the 1 h group, but no such increase was observed in the brain. Rather, brain tissue samples showed an increase in MMP-9 within the 48 h group. This suggests that early increases in MMP-9 are due to peripherally derived sources outside the CNS, such as mononuclear blood cells, PMN leukocytes, and endothelial cells lining the vasculature (Gidday *et al*, 2005; Romanic *et al*, 1998; Wang *et al*, 2009). In contrast, the increase in MMP-9 in brain tissue more strongly supports a local inflammatory response, in which brain and blood-derived macrophages participate in clearing cellular debris (Bergeron *et al*, 1997). Interestingly, plasma MMP-2 changed in the opposite direction of tissue MMP-2. Although we were only able to observe a decreasing trend with zymography, ELISA showed a significant decrease in plasma MMP-2 within the 48 h group (data not shown). One potential explanation for this decrease is neurovascular remodeling of the extracellular matrix and basal lamina, a dynamic process that requires MMP-2. If this process were to take place beyond normal rates, it is feasible that the intravascular pool of MMP-2 could be depleted. The concomitant increase in MMP-2 in brain tissue again supports the theory of active vascular remodeling within the infarct (Slevin *et al*, 2009), and may account for the increased passage of Gd-DTPA into the brain parenchyma at 48 h.

Our observations of an early increase in plasma MMP-9 and delayed increases in tissue MMP-2 and MMP-9 are in contrast to recent experimental work (Nagel *et al*, 2008; Park *et al*, 2009). The early increase in plasma MMP-9 in the 1 h group and the restoration to sham/naive levels at 24 and 48 h is most likely due to the presence of reperfusion in our model. This finding highlights an important difference found between the levels of MMPs within permanent occlusion models and reperfusion models of experimental stroke. As we did not measure plasma MMP levels before reperfusion, we cannot say whether the MMP levels at that particular time point would have been elevated and comparable to that of permanent MCAO. In the clinical setting, it will be imperative to keep track of the patient's reperfusion status and measured levels of MMPs within the blood. Patients without any reperfusion or partial reperfusion may show a different temporal pattern of MMP release in the blood in comparison to patients with full reperfusion.

Another source that may contribute to the differences between our observations and that of prior study includes the species and strain of animal chosen for experimental stroke modeling (Spiers *et al*, 2005; Tagaya *et al*, 1997). We used the SHR rat, a strain that has genetic hypertension and which is known for increased stroke severity, edema, and hemorrhage in comparison to their normotensive counterparts (Barone *et al*, 1992; Henning *et al*, 2008*a*). We observed a higher than expected level of active MMPs in the blood in SHR, even in naive animals receiving no surgical intervention and minimal exposure to anesthesia. This may be related to inherent changes in vascular function and signaling at the level of the endothelium (Spiers *et al*, 2005). To ascertain the impact of hypertension on MMP regulation and BCSFB-BBB disruption, a comparison between WKY and SHR under the same experimental conditions presented here would be required.

It is also important to consider that MMPs measurements may differ slightly based on zymo-

graphy methods, choice of anesthetics, stress levels, etc. We measured MMP levels using standard zymography for blood, and zymography according to gelatin sepharose purification for brain tissue (Zhang and Gottschall, 1997). For brain tissue, we observed an ~10-fold amplification in MMP signal using the purification method, without augmenting active MMP levels. This was based on the comparison of pro and active forms of MMPs with and without purification. Our measurements for both plasma and tissue MMPs were optimized based on serial dilutions of protein samples in order to be in the linear range. We measured total MMP levels, as well as pro and active MMP levels, to determine the relative signal changes in MMP-2 and MMP-9 in the plasma and brain tissue. However, we did not determine the protein yield. For quantification of exact protein yield rather than relative measures of MMPs, we direct you to the methods presented by Heo *et al* (1999).

Unique to this study, we found that each anatomical pattern of barrier disruption identified on post-contrast FLAIR is linked to a specific source of MMPs. Post-contrast FLAIR identification of ventricular enhancement in the 1 h group and an increase in plasma MMP-9 levels are strongly suggestive of an association between acute BCSFB disruption and plasma MMP-9. Post-contrast FLAIR identification of parenchymal enhancement in the 48 h group and an increase in brain tissue levels of both MMP-2 and MMP-9 are strongly suggestive of an association between delayed BBB disruption and tissue MMP levels. The changes that occur between these two states of barrier disruption represent important pathological changes that may identify an opportunistic window for neuroprotective strategies, such as MMP inhibition. Understanding the dynamic nature of MMP-2 and MMP-9 after brain ischemia is important in developing novel adjunct stroke therapies to recombinant tPA. Our findings support the therapeutic rationale of using MMP-9 inhibitors during the acute phase of ischemic stroke, alone or in conjunction with tPA administration. Future studies should focus on understanding the effectiveness of inhibitor therapies at different time points after ischemia in relation to BBB disruption and MMP levels. In addition, elucidating the mechanism(s) of the early BCSFB disruption at the level of the choroid plexus promises to be an exciting area for future study. The combination of imaging markers, such as post-contrast FLAIR, and blood biomarkers, such as MMPs, offer a unique and powerful tool for improved translations from bench to the bedside and future clinical stroke studies.

Acknowledgements

This research was supported by the Division of Intramural Research of the National Institute of Neurological Disorders and Stroke, National Institutes of Health. We acknowledge the technical assistance of Paola Castri, PhD, Yang-Ja Lee-Wickner, PhD, and Christina Stuelten, PhD.

Conflict of interest

The authors declare no conflict of interest.

References

Barone FC, Price WJ, White RF, Willette RN, Feuerstein GZ (1992) Genetic hypertension and increased susceptibility to cerebral ischemia. *Neurosci Biobehav Rev* 16: 219–33

Bergeron M, Ferriero DM, Vreman HJ, Stevenson DK, Sharp FR (1997) Hypoxia-ischemia, but not hypoxia alone, induces the expression of heme oxygenase-1 (HSP32) in newborn rat brain. *J Cereb Blood Flow Metab* 17:647–58

del Zoppo GJ, Milner R, Mabuchi T, Hung S, Wang X, Berg GI, Koziol JA (2007) Microglial activation and matrix protease generation during focal cerebral ischemia. *Stroke* 38:646–51

Ennis SR, Keep RF (2006) The effects of cerebral ischemia on the rat choroid plexus. *J Cereb Blood Flow Metab* 26:675–83

Garcia JH, Wagner S, Liu KF, Hu XJ (1995) Neurological deficit and extent of neuronal necrosis attributable to middle cerebral artery occlusion in rats. Statistical validation. *Stroke* 26:627–35

Gidday JM, Gasche YG, Copin JC, Shah AR, Perez RS, Shapiro SD, Chan PH, Park TS (2005) Leukocyte-derived matrix metalloproteinase-9 mediates blood-brain barrier breakdown and is proinflammatory after transient focal cerebral ischemia. *Am J Physiol Heart Circ Physiol* 289:H558–68

Hamann GF, Okada Y, del Zoppo GJ (1996) Hemorrhagic transformation and microvascular integrity during focal cerebral ischemia/reperfusion. *J Cereb Blood Flow Metab* 16:1373–8

Hamann GF, Okada Y, Fitridge R, del Zoppo GJ (1995) Microvascular basal lamina antigens disappear during cerebral ischemia and reperfusion. *Stroke* 26:2120–6

Henning EC, Latour LL, Hallenbeck JM, Warach S (2008*a*) Reperfusion-associated hemorrhagic transformation in SHR rats: evidence of symptomatic parenchymal hematoma. *Stroke* 39:3405–10

Henning EC, Latour LL, Warach S (2008*b*) Verification of enhancement of the CSF space, not parenchyma, in acute stroke patients with early blood-brain barrier disruption. *J Cereb Blood Flow Metab* 28:882–6

Heo JH, Lucero J, Abumiya T, Koziol JA, Copeland BR, del Zoppo GJ (1999) Matrix metalloproteinases increase very early during experimental focal cerebral ischemia. *J Cereb Blood Flow Metab* 19:624–33

Johanson CE, Palm DE, Primiano MJ, McMillan PN, Chan P, Knuckey NW, Stopa EG (2000) Choroid plexus recovery after transient forebrain ischemia: role of growth factors and other repair mechanisms. *Cell Mol Neurobiol* 20:197–216

Kastrup A, Engelhorn T, Beaulieu C, de Crespigny A, Moseley ME (1999) Dynamics of cerebral injury, perfusion, and blood-brain barrier changes after temporary and permanent middle cerebral artery occlusion in the rat. *J Neurol Sci* 166:91–9

Koizumi J, Yoshida Y, Nakazawa T, Ooneda G (1986) Experimental studies of ischemic brain edema. I. A new experimental model of cerebral embolism in rats in which recirculation can be introduced in the ischemic area. *Jpn J Stroke* 8:1–8

Latour LL, Kang DW, Ezzeddine MA, Chalela JA, Warach S (2004) Early blood-brain barrier disruption in human focal brain ischemia. *Ann Neurol* 56:468–77

Lee SR, Kim HY, Rogowska J, Zhao BQ, Bhide P, Parent JM, Lo EH (2006) Involvement of matrix metalloproteinase in neuroblast cell migration from the subventricular zone after stroke. *J Neurosci* 26:3491–5

Lo EH, Pan Y, Matsumoto K, Kowall NW (1994) Blood-brain barrier disruption in experimental focal ischemia: comparison between *in vivo* MRI and immunocytochemistry. *Magn Reson Imaging* 12:403–11

Longa EZ, Weinstein PR, Carlson S, Cummins R (1989) Reversible middle cerebral artery occlusion without craniectomy in rats. *Stroke* 20:84–91

Mamourian AC, Hoopes PJ, Lewis LD (2000) Visualization of intravenously administered contrast material in the CSF on fluid-attenuated inversion-recovery MR images: an *in vitro* and animal-model investigation. *AJNR Am J Neuroradiol* 21:105–11

Milner R, Hung S, Wang X, Berg GI, Spatz M, del Zoppo GJ (2008) Responses of endothelial cell and astrocyte matrix-integrin receptors to ischemia mimic those observed in the neurovascular unit. *Stroke* 39:191–7

Mitchell K, Yang HY, Berk JD, Tran JH, Iadarola MJ (2009) Monocyte chemoattractant protein-1 in the choroid plexus: a potential link between vascular pro-inflammatory mediators and the CNS during peripheral tissue inflammation. *Neuroscience* 158:885–95

Montaner J, Alvarez-Sabin J, Molina C, Angles A, Abilleira S, Arenillas J, Gonzalez MA, Monasterio J (2001*a*) Matrix metalloproteinase expression after human cardioembolic stroke: temporal profile and relation to neurological impairment. *Stroke* 32:1759–66

Montaner J, Alvarez-Sabin J, Molina CA, Angles A, Abilleira S, Arenillas J, Monasterio J (2001*b*) Matrix metalloproteinase expression is related to hemorrhagic transformation after cardioembolic stroke. *Stroke* 32:2762–7

Mun-Bryce S, Rosenberg GA (1998) Matrix metalloproteinases in cerebrovascular disease. *J Cereb Blood Flow Metab* 18:1163–72

Murata Y, Rosell A, Scannevin RH, Rhodes KJ, Wang X, Lo EH (2008) Extension of the thrombolytic time window with minocycline in experimental stroke. *Stroke* 39:3372–7

Nagahiro S, Goto S, Korematsu K, Sumi M, Takahashi M, Ushio Y (1994) Disruption of the blood-cerebrospinal fluid barrier by transient cerebral ischemia. *Brain Res* 633:305–11

Nagel S, Su Y, Horstmann S, Heiland S, Gardner H, Koziol J, Martinez-Torres FJ, Wagner S (2008) Minocycline and hypothermia for reperfusion injury after focal cerebral ischemia in the rat: effects on BBB breakdown and MMP expression in the acute and subacute phase. *Brain Res* 1188:198–206

Palm D, Knuckey N, Guglielmo M, Watson P, Primiano M, Johanson C (1995) Choroid plexus electrolytes and ultrastructure following transient forebrain ischemia. *Am J Physiol* 269:R73–9

Park KP, Rosell A, Foerch C, Xing C, Jean Kim W, Lee S, Opdenakker G, Furie KL, Lo EH (2009) Plasma and brain matrix metalloproteinase-9 after acute focal cerebral ischemia in rats. *Stroke* 40:2836–42

Romanic AM, White RF, Arleth AJ, Ohlstein EH, Barone FC (1998) Matrix metalloproteinase expression increases after cerebral focal ischemia in rats: inhibition of matrix metalloproteinase-9 reduces infarct size. *Stroke* 29:1020–30

Rosell A, Alvarez-Sabin J, Arenillas JF, Rovira A, Delgado P, Fernandez-Cadenas I, Penalba A, Molina CA, Montaner J (2005) A matrix metalloproteinase protein array reveals a strong relation between MMP-9 and MMP-13 with diffusion-weighted image lesion increase in human stroke. *Stroke* 36:1415–20

Rosell A, Lo EH (2008) Multiphasic roles for matrix metalloproteinases after stroke. *Curr Opin Pharmacol* 8:82–9

Rosenberg GA (2002) Matrix metalloproteinases in neuroinflammation. *Glia* 39:279–91

Rosenberg GA, Navratil M, Barone F, Feuerstein G (1996) Proteolytic cascade enzymes increase in focal cerebral ischemia in rat. *J Cereb Blood Flow Metab* 16:360–6

Simard JM, Kent TA, Chen M, Tarasov KV, Gerzanich V (2007) Brain oedema in focal ischaemia: molecular pathophysiology and theoretical implications. *Lancet Neurol* 6:258–68

Slevin M, Krupinski J, Rovira N, Turu M, Luque A, Baldellou M, Sanfeliu C, de Vera N, Badimon L (2009) Identification of pro-angiogenic markers in blood vessels from stroked-affected brain tissue using laser-capture microdissection. *BMC Genomics* 10:113

Sood RR, Taheri S, Candelario-Jalil E, Estrada EY, Rosenberg GA (2008) Early beneficial effect of matrix metalloproteinase inhibition on blood-brain barrier permeability as measured by magnetic resonance imaging countered by impaired long-term recovery after stroke in rat brain. *J Cereb Blood Flow Metab* 28:431–8

Spiers JP, Kelso EJ, Siah WF, Edge G, Song G, McDermott BJ, Hennessy M (2005) Alterations in vascular matrix metalloproteinase due to ageing and chronic hypertension: effects of endothelin receptor blockade. *J Hypertens* 23:1717–24

Sumii T, Lo EH (2002) Involvement of matrix metalloproteinase in thrombolysis-associated hemorrhagic transformation after embolic focal ischemia in rats. *Stroke* 33:831–6

Tagaya M, Liu KF, Copeland B, Seiffert D, Engler R, Garcia JH, del Zoppo GJ (1997) DNA scission after focal brain ischemia. Temporal differences in two species. *Stroke* 28:1245–54

Wang G, Guo Q, Hossain M, Fazio V, Zeynalov E, Janigro D, Mayberg MR, Namura S (2009) Bone marrow-derived cells are the major source of MMP-9 contributing to blood-brain barrier dysfunction and infarct formation after ischemic stroke in mice. *Brain Res* 1294:183–92

Warach S, Latour LL (2004) Evidence of reperfusion injury, exacerbated by thrombolytic therapy, in human focal brain ischemia using a novel imaging marker of early blood-brain barrier disruption. *Stroke* 35:2659–61

Zhang JW, Gottschall PE (1997) Zymographic measurement of gelatinase activity in brain tissue after detergent extraction and affinity-support purification. *J Neurosci Methods* 76:15–20

Zhao BQ, Wang S, Kim HY, Storrie H, Rosen BR, Mooney DJ, Wang X, Lo EH (2006) Role of matrix metalloproteinases in delayed cortical responses after stroke. *Nat Med* 12:441–5